International Journal of Automotive Technology, Vol. 6, No. 1, pp. 45–52 (2005)

1229-9138/2005/019-07

EFFECT OF HARDNESS CHANGES AND MICROSTRUCTURAL DEGRADATION ON CREEP BEHAVIOR OF A Mod.9Cr-1Mo STEEL

K.-S. PARK[1)*], H.-S. CHUNG[2)], K.-J. LEE[3)],
Y.-G. JUNG[4)], C.-Y. KANG[5)] and T. ENDO[1)]

[1)]Department of Mechnical Engineering and Materials Science, Yokohama National University, Yokohama, Japan
[2)]School of Mechanical and Aerospace Engineering, Gyeongsang National University, Gyeongnam 650-160, Korea
[3)]Division of Information Commmunication, Yangsan College, Gyeongnam 626-740, Korea
[4)]School of Mechnical Engineering, Kumoh National Institute of Technology, Gyeongbuk 730-701, Korea
[5)]Division of Materials Science and Engineering, Bukyung National University, Busan 608-739, Korea

(Received 16 October 2003; Revised 29 March 2004)

ABSTRACT–Interrupted creep tests for investigating the structural degradation during creep were conducted for a Mod.9Cr-1Mo steel in the range of stress from 71 to 167 MPa and temperature from 873 to 923 K. The change of hardness and tempered martensitic lath width was measured in grip and gauge parts of interrupted creep specimens. The lath structure was thermally stable in static conditions. However, it was not stable during creep, and the structural change was enhanced by creep strain. The relation between the change in lath width and creep strain was described quantitatively. The change in Vickers hardness was expressed by a single valued function of creep LCR(life consumption ratio). Based on the empirical relation between strain and lath width, a model was proposed to describe the relation between change in hardness and creep LCR. The comparison of the model with the empirical relation suggests that about 65% of hardness loss is due to the decrease of dislocation density accompanied by the movement of lath boundaries. The role of precipitates on subboundaries was discussed in connection with the abnormal subgrain growth appearing in low stress regime.

KEY WORDS : Creep, Creep life, Life assessment, Lath width, Hardness, Subgrain

1. INTRODUCTION

Mod.9Cr-1Mo steel (T91) is one of the ferritic heat resistant steels used widely for fossil power plants because of its excellent high temperature strength and the advantage of small thermal stress in cyclic operations. As a results, long-term service aged components are now growing, and the elaboration of life assessment technology is demanded for this material. In order to meet the requirements for creep life assessment, studies on the constitutive equations (Park *et al.*, 1998, 1999, 2001), the substructural evolution (Sawada *et al.*, 1997; 1998; 1999), the growth of precipitates during creep (Cerri *et al.*, 1998), and also the relation between creep strength and structures (Masuyama and Nishimura, 1994; Orlova *et al.*, 1998; Kushima *et al.*, 1999; Suzuki *et al.*, 2000) have been investigated. Among these works, the observation reported by Kushima *et al.* (1999) is worthy of attention.

They found that the decrease in creep life and rupture strain, which emerged when creep life exceeded 10,000 hrs, was associated with abnormal subgrain growth occurring in the vicinity of prior austenite grain boundaries. To investigate this phenomenon more closely, Suzuki *et al.* (2000) studied the precipitates near prior austenite grain boundaries, and found Z phase particles growing rapidly at the sacrifice of fine MX particles containing Nb and V. Based on their observations, they ascribed the abnormal subgrain growth to the Z phase particles appearing preferentially near prior austenite grain boundaries.

Their new finding is quite important in understanding the loss of creep strength in long term creep. However, the structural evolution in short term creep is also important to deepen the understanding of structural degradation. In the present paper, the change of hardness and tempered martensitic lath width, and also the relation among hardness, creep life and lath width will be treated quantitatively, followed by discussion on the structural evolution and the non-homogeneous recovery of lath structure appearing in low stress regimes.

**Corresponding author.* e-mail: kspark@hotmail.com

2. EXPERIMENTAL PROCEDURE

The heat treatment applied to an as-received Mod. 9Cr-1Mo steel (ASME SA-213 T-91) was normalization at 1313 K for 1 hr and tempering at 1053 K for 2 hrs. The chemical compositions of the material are show in Table 1. Two series of interrupted creep tests, A and B, were conducted at atmospheric pressure. Creep specimens with two shoulders in both ends had a gauge part of 30 mm in length and 6 mm in diameter. The stress and temperature for series A were 157 to 186 MPa and 873 to 898 K, respectively, and those for series B were 71 to 115 MPa and 873 to 923 K, respectively. In series A tests, strain-time relations were automatically recorded. The measurements of ambient hardness and TEM observation were carried out on the gauge and grip parts of interrupted specimens. The load applied for the Vickers hardness measurements was 2 kg for 30 s. The initial hardness (H_0) was 225 and 214 for series A and B, respectively. In series B tests, only the hardness measurements were conducted, and the creep curve was not recorded. The longest creep life of series A was 1,185 hrs, and that of series B was 18,736 hrs.

3. EXPERIMENTAL RESULTS

3.1. Change in Vickers Hardness due to Creep

Examples of interrupted and uninterrupted creep curves

Table 1. Chemical composition in mass%.

C	Si	Mn	P	S	Ni
0.1	0.25	0.4	0.016	0.005	0.04
Cr	Mo	Nb	Al	V	N
8.4	0.9	0.07	0.005	0.21	0.044

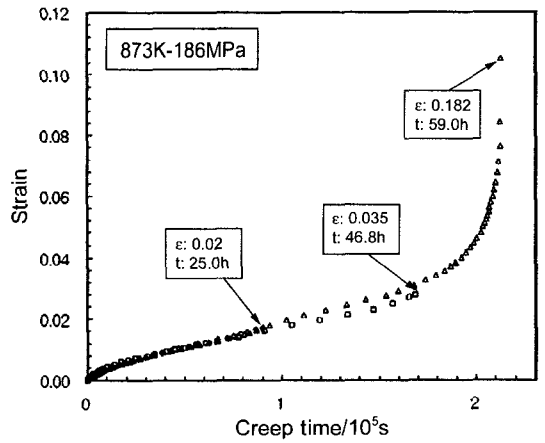

Figure 1. An example of interrupted and uninterrupted creep curves tested at 186 MPa and 873 K.

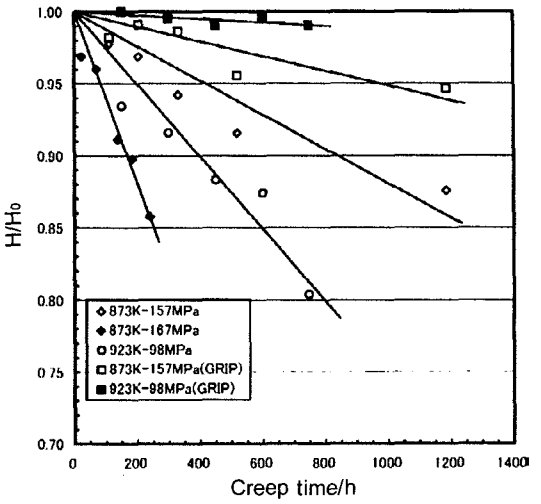

Figure 2. Change in Vickers hardness ratio (H/H_0) with creep time for the interrupted specimens whose interruption time is from 22.4 to 1185 hours, where H_0 and H are the ambient hardness before and after creep interruption, respectively.

are shown in Figure 1 in which interrupted time and strain are given. These creep curves are characterized by a relatively long primary creep common to tempered martensitic structure steels (Park *et al.*, 1998). The measurements of Vickers hardness were carried out on the grip and gauge parts of crept specimens. For the convenience of description, the change in hardness ratio (H/H_0) from 22.4 to 1,185 hrs and that of 657 to 18,736 hrs are shown separately as a function of time in Figures

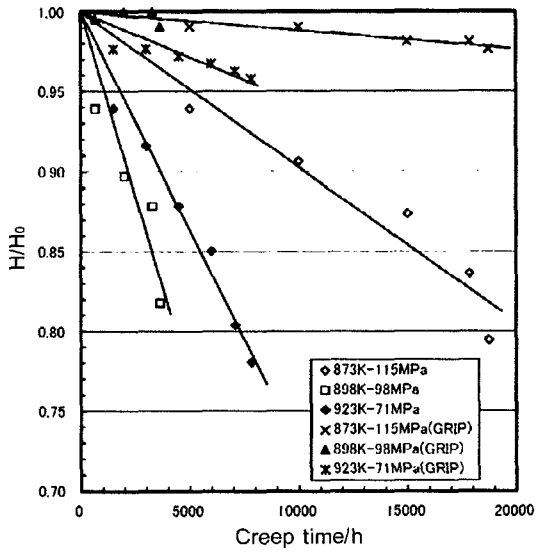

Figure 3. Change in Vickers hardness ratio(H/H_0) with creep time for the interrupted specimens whose interruption time is from 657 to 18736 hours.

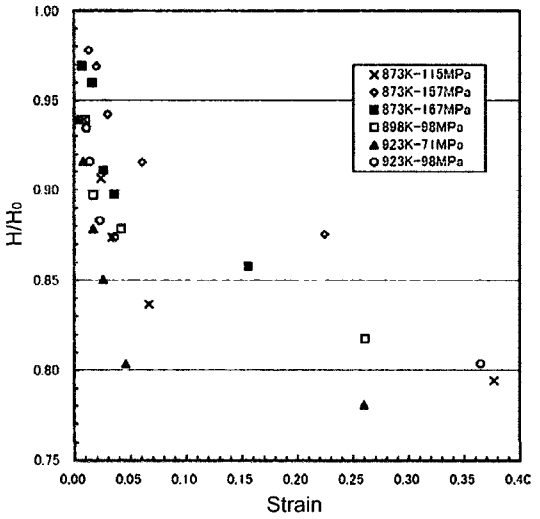

Figure 4. Relation between the change in hardness ratio and creep strain.

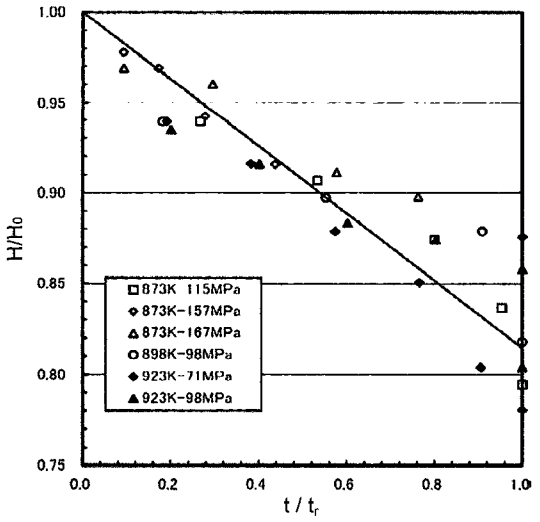

Figure 5. Relation between the change in hardness ratio and life consumption ratio (t/t_r).

2 and 3. The decrease in hardness ratio can be expressed approximately by a linear relation of time, although the slope of the lines depends on creep conditions.

It should be noted that the decrease of hardness is much smaller in the grip parts than in the gauge parts. This clearly demonstrates that the as- received structures are thermally stable if strain is not applied to the material (Park *et al.*, 1999). The relation between hardness change and strain is depicted in Figure 4. The figure shows that the change in hardness is greater in the case of smaller strains. The relation between hardness ratio and life consumption ratio (LCR), normalized time divided by the corresponding creep life t_r, is shown in Figure 5.

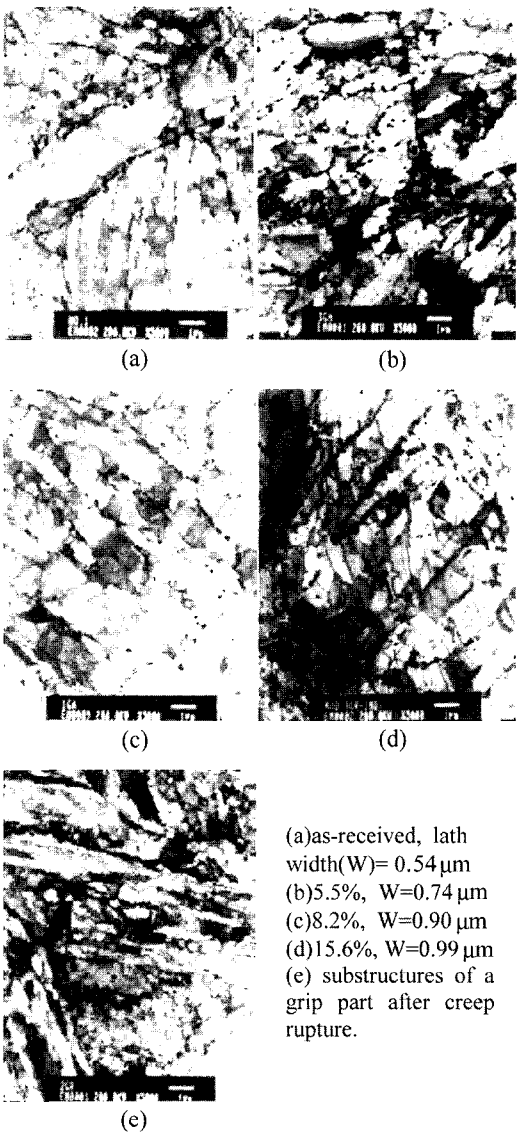

(a)as-received, lath width(W)= 0.54 μm
(b)5.5%, W=0.74 μm
(c)8.2%, W=0.90 μm
(d)15.6%, W=0.99 μm
(e) substructures of a grip part after creep rupture.

Figure 6. TEM micrograph showing the change of the tempered martensitic structures with creep strain. Testing stress and temperature are 167 Mpa and 873 K, respectively.

Although there is some scattering as LCR approaches unity, the hardness ratio can be expressed as a function of LCR as below;

$$H/H_0 = 1-0.19(t/t_r) \quad (1)$$

3.2. Lath Structures of Interrupted Specimens

As described in the previous section, Vickers hardness in the gauge parts decreases with increase in LCR. Structural observation was carried out by TEM on interrupted creep specimens. Figure 6(a) shows the microstructure of an as-received specimen. The micrograph shows a

randomly oriented lath structure, and the lath width of an as-received specimen was about 0.54 μm. There remain the densely populated dislocations within lath boundaries introduced in martensitic transformation, and many carbidies are also seen along prior austenite, packet, block or lath boundaries. Their shape and size suggest that carbides are mostly of $M_{23}C_6$ type. Figures 6(b) to 6(d) show the microstructures of the gauge parts tested at 873 K and 167 MPa. The interrupted creep strains are given in these figures. It is to be noted that the lath width increases continuously with increaing creep strain, and the shape of the lath structure changes gradually from an initial rectangular shape to a round one. As Sawada *et al.* (2000) showed, dislocation density within lath boundaries decreases gradually as the creep strain increases. In some cases we could not identify the lath boundary even if the precipitates lined up clearly. These lined-up precipitates indicate the position where the lath boundary was located before creep. Figure 6(e) shows the substructures of the grip part, which are similar to those of the as-received specimens and dissimilar to those of the gauge parts. Actually, the lath width of grip parts after rupture was about 0.55 μm which was close to the initial lath width. This fact corresponds to the smaller change in hardness in the grip parts and supports the speculation that the decrease in hardness of the gauge section is due to the decrease of the dislocation density caused by the migration of the lath boundaries.

3.3. Change in Lath Width with Creep Deformation

Since the lath width increases with strain, the measurements of lath width were carried out. The lath was rectangular shape in an initial state but changed to an equi-axed round one in the late stage of creep. In the present study, the distance between the shorter sides of a rectangle was taken as the lath width, and the diameter was taken for the round subgrains. The results of

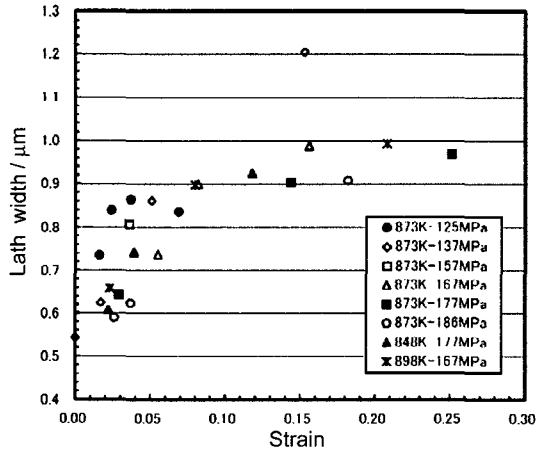

Figure 7. Lath width as a function of creep strain.

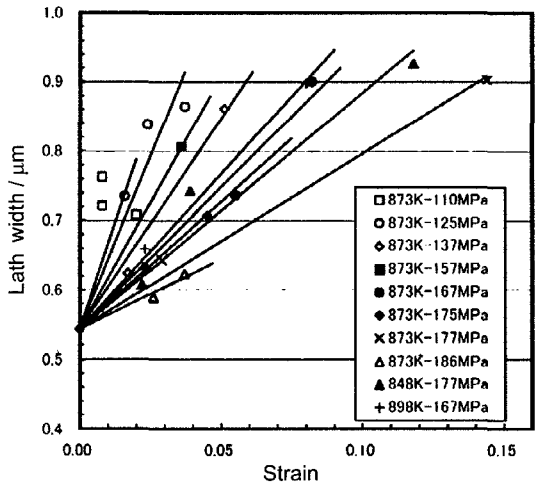

Figure 8. Plot of lath width against creep strain by omitting the data near rupture strain.

measured lath width are plotted against strain along with the results reported by other investigators (Sawada *et al.*, 1999; Orlova *et al.*, 1998; Suzuki *et al.*, 2000) in Figure 7. It is clear that the lath width increases with strain and the rate of increase in lath width, $dW/d\varepsilon$, becomes small as strain approaches rupture strain. It is necessary to emphasize here that creep rupture is rupture is generally associated with a local necking. In such a case, the nominal rupture strain is usually much larger than the true strain subjected to a foil sample for TEM study since the foil is taken from the gauge section well apart from the necking region. This is probably the reason why $dW/d\varepsilon$ becomes smaller as strain approaches creep rupture. From this standpoint, the lath width is plotted against strain in Figure 8 where the data near rapture strain are omitted. The figure shows the tendency for W to change linearly with strain, and the slope of the lines depend on the stress when compared at about the same temperature. From Figure 8, the change in lath width is expressed as follows;

$$\Delta W = \beta\varepsilon \tag{2}$$

where β is the slope of the lines.

4. DISCUSSION

4.1. Stress and Strain Dependence of Lath Width

It is clear that the slope of the lines in Figure 8 depends on stress. However, taking into account that the lath width approaches a constant value depending solely on stress, it is rather natural that the slope of the line depends on stress, since the lath width approaches a smaller value at higher stresses. Therefore, the values of ΔW divided by $(W_s - W_o)$ are shown as a function of strain in Figure 9, where W_o is the initial lath width, and W_s is the final lath

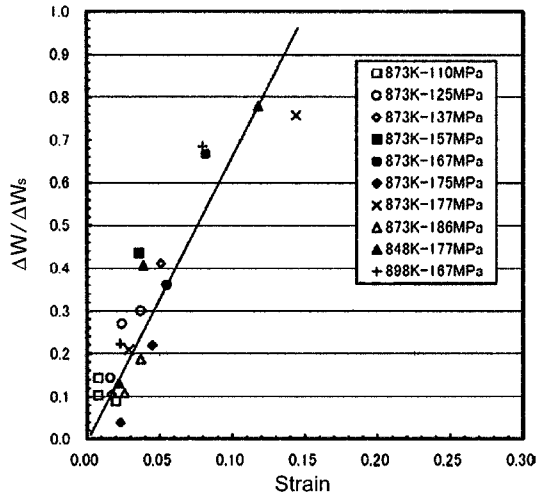

Figure 9. Relation between ΔW divided by $(W_s - W_o)$ and creep strain, where W_o is the initial lath width, and W_s is the final lath width depending sloply on stress.

width depending solely on stress. There is some scattering in plots, but all data points lay around a single line with the slope independent of stress and temperature. From this figure, ΔW can be expressed as below;

$$\Delta W = \alpha(W_S - W_o)\varepsilon \tag{3}$$

where α is the constant of the magnitude of about 6.7 μm.

4.2. Evolution of Lath Structure

As mentioned above, the structural observation in the grip parts shows that the lath structure does not evolve substantially. This suggests that the subboundaries are pinned with precipitates, and they cannot move easily without the influence of creep strain. However, once they escape from precipitates with the aid of stress and temperature, they can move and evolve readily making use of interfacial energy as a driving force for subgrain growth. Therefore, the growth process of lath structure will be treated in analogy with the grain growth (Hillert, 1965) associated with the decrease of total interfacial energy.

$$dW/dt = k\Gamma(1/W - 1/W_S) \tag{4}$$

where k is the proportional constant, Γ is the interfacial energy. When W_S is close to W_o, Equation (4) can be rewritten as,

$$dW/dt = k\Gamma(1/W_S - 1/W_o)(W_S W_o) \tag{5}$$

Since the lath boundary is composed of dislocations introduced in martensitic transformation, the energy for lath boundary can be expressed in the form of a small angle boundary (Read, 1953) as below:

$$\Gamma \cong A\theta(\ln B - \ln\theta) \cong A\theta \cong Ab/h \tag{6}$$

where θ is the tilt angle of the boundary, A and B are constants, h is the separation between dislocations in the subboundaries, and b is the strength of Burgers vector. As Equation (6) shows, the interfacial energy Γ is proportional to the spacing between dislocations, h. Therefore, interfacial energy is expected to increase as the number of dislocations entering into lath boundaries increases.

Hereafter, densely populated dislocations within lath structures shall be classified into three categories, (1) a dislocation group which is bounded weakly by other dislocations or precipitates, (2) a dislocation group bounded moderately, and (3) a dislocation group bounded strongly with other dislocations and precipitates. Dislocations in the first category are expected to move relatively easily in the early stage of creep, and they contribute to the large primary creep common to tempered martensite structure materials. Dislocations in the second category begin to move following the dislocations in the first category. Since they can travel a relatively large distance, they contribute to creep strain and the increase of lath boundary energy by entering into the subboundaries. As speculated above, the dislocation motion is quite complicated, however, dislocations in the second category will be considered for the sake of simplicity.

The dislocations in the second category are probably generated from tangled dislocations. So the dislocation density in the second category is expected to be proportional to the generation rate of dislocations $\dot{\rho}$ released from dislocation tangles. On the other hand, since the strain rate is proportional to the generation rate of dislocations $\dot{\rho}$, the lath boundary energy can be replaced by the strain rate. Taking this into consideration, Equation (5) can be rewritten as;

$$dW/dt = k'\dot{\varepsilon}(W_S - W_o) \tag{7}$$

where, k' is a constant. From Equation (7) following equation is obtained;

$$dW = k'(W_S - W_o)\varepsilon \tag{8}$$

It is to be noted that Equation (8) is similar to Equation (3).

In the deduction of Equation (8), we assumed that the W is close to W_o. However, Equation (8) holds even if the magnitude of W is twice as larger as that of W_o. This is probably because the interfacial energy is not constant all the way to rupture, but it is expected to increase in the late stage of creep because of increased dislocations entering into lath boundaries.

4.3. Relation between Hardness and LCR

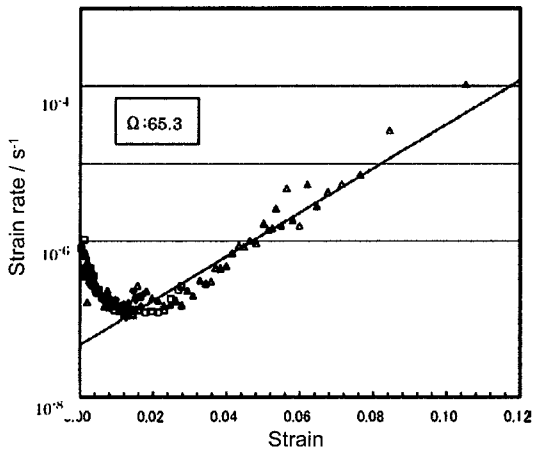

Figure 10. Relation between logarithm of strain rate and ture strain corresponding to Figure 1.

As-received tempered martensitic structure steels have high dislocation density, but the dislocation density decreases during creep and leads to structural degradation. At the present time, it is not clear what kind of mechanisms are operating in dislocation annihilation. In this section, an attempt will be made to explain the hardness loss in connection with the migration of subboundaries.

Let us suppose that lath boundaries migrate by ΔW during creep and that they absorb all the dislocations behind them. In this case, the average dislocation density (ρ) can be expressed as below;

$$\rho = \rho_0(W_o/W)^2 \tag{9}$$

where ρ_0 is the initial dislocation density.

Since the hardness at ambient temperature is expected to be proportional to the square root of dislocation density, Equation (10) results from Equations (3) and (9) as;

$$H-H_0 = [(W_o-W)/W]H_0 = -[(W_S-W_o)/W]6.7\varepsilon H_0 \tag{10}$$

In order to relate Equation (10) with the empirical Equation (1), an attempt will be made to relate LCR with creep strain. Figure 10 shows the relation between the logarithm of the strain rate and true strain corresponding to Figure 1. It is clear that the logarithm of the strain rate changes linearly with true strain over a relatively wide range. Therefore, the following equation (Sandstrom and Konyr, 1972; Endo and Shi, 1994; Prager, 1994) holds.

$$\ln\dot{\varepsilon} = \ln\dot{\varepsilon}_0 + \Omega\varepsilon \tag{11}$$

where ε is the instantaneous strain rate, $\dot{\varepsilon}_0$ is the imaginary initial strain rate, and Ω is the slope of the line (strain rate acceleration factor). Assuming that Equation (11) holds over an entire rage of creep, creep life is

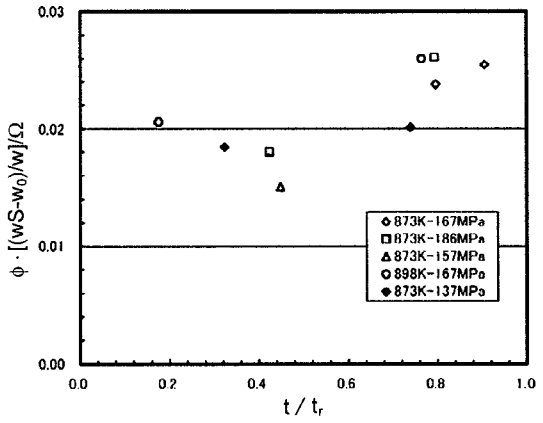

Figure 11. Relation between the magnitude within the bravkets of Equation (16) and LCR, (t/t_r).

expressed by Equation (12) (Endo and Shi, 1994; Prager, 1994). One can obtain creep strain by integrating Equation (11) with respect to time and making use of Equation (12).

$$t_r = 1/(\Omega\dot{\varepsilon}_0) \tag{12}$$

$$\varepsilon = (1/\Omega)\ln[1/(1-t/t_r)] \tag{13}$$

Equation (13) can be rewritten in the form;

$$\varepsilon \cong \Psi(1/\Omega)(t/t_r) \tag{14}$$

where Ψ is given by Equation (15).

$$\Psi = \ln[1/(1-(t/t_r))]/(t/t_r) \tag{15}$$

Comparison of Equations (14) and (15) shows that the magnitude of Ψ is unity at $t = 0$, and it increases up to about 7.

Using Equation (14), Equation (10) is rewritten in the form as:

$$\frac{H}{H_0} = 1 - 6.7[(1/\Omega)\{(W_S - W_0)/W\}\Psi](t/t_r) \tag{16}$$

Figure 11 shows the relation between the magnitude within the brackets of Equation (16) and LCR. The magnitude of Ω depends on stress and slightly on temperature (Park *et al.*, 1998). However, its magnitude is about 64 in the present case. There is some scattering, but the magnitude within the brackets of Equation (16) is a constant of about 0.02, so that the magnitude of the term in front of t/t_r in Equation (16) is about 0.13 which is about 65% of 0.19 in Equation (1). This means that about 65% of dislocations within lath structures are absorbed and eliminated by the movement of lath boundaries, and the rest of the dislocations are annihilated by other mechanisms such as mutual annihilation due to the motion of isolated and moderately bounded dislocations.

4.4. Non-homogenious Recovery of Lath Structures

When creep duration exceeds 10,000 hrs, creep life becomes shorter than the extrapolated from the short time creep data, and that rupture strain also becomes smaller (Suzuki *et al.*, 2000; ISIJ, 1992). Since the recent study (Suzuki *et al.*, 2000) showed that this phenomenon had something to do with the non-homogeneous recovery of lath structures and the appearance of the Z phase, we will discuss this phenomenon in connection with the knowledge obtained in the present study. As-received Mod.9Cr-1Mo steel exhibits tempered martensitic structures containing prior austenite, packet, block and lath boundaries. Their boundaries are decorated by carbides such as $M_{23}C_6$ and MX that appeared in the tempering process. This is the reason why the substructure is thermally stable in the grip parts. However, lath boundaries can move relatively easily under the influence of stress, and as a result, the dislocation density and hardness decrease readily in accordance with the lath boundary movement. In other words, subboundaries are supposed to be released from the pinning of carbides in the early stage of creep under the action of stress. Hereafter, stress needed for a sub boundary to unlock the pinning of carbides will be discussed.

Since the lath boundaries are composed of a group of dislocations which is introduced to relax the stress due to martensitic transformation, they can glide under the action of stress at elevated temperatures. Actually, there are some reports demonstrating the subboundary migration and its contribution to total creep strain (Excell and Warrington, 1972; Fukutomi and Horiuchi, 1979; Fukutomi and Horiuchi, 1981). Let us suppose the subboundary along which precipitates of the size R are arranged at the intervals of precipitates Λ. Since the work necessary to move the subboundary by a distance $R/2$ is equal to the increase in interfacial energy due to the escape from precipitates on the boundary (Nishizawa *et al.*, 1977), the stress required to detach the subboundary from precipitates is as follows;

$$\tau = \pi\Gamma Rh/\Lambda^2 b \tag{17}$$

where h is the separation between dislocations composed of subboudaries, and Γ is the interfacial energy of lath boundary. On the other hand, Γ is expected to be of the form, $\Gamma = \alpha\, Gb^2/h$, where α is the constant of the magnitude of about 0.5, G is the shear modulus, and b is the Burgers vector. Accordingly, the tensile stress needed to release a subboundary from the constraint of the precipitates is as below;

$$\sigma = \alpha M\, \pi GbR/\Lambda^2 \tag{18}$$

where M is the Taylor factor. Suzuki *et al.* (2000) observed the precipitates along lath boundaries by filtered electron microscopy and showed that the magnitudes of Λ and R are about 500 nm and 50 to 2000 nm, respectively. Taking the values of G (= 6245 MPa), b (= 24.8 nm), α (= 0.5), M (= 2.0), and Λ = 500 nm and R = 1000 nm, the maginitude of σ was estimated crudely to be 100 MPa. The stress level in the present study is more than 100 MPa so that the assumption that the subboundary is free from the locking of precipitates appears reasonable. In contrast to the present study, Suzuki *et al.* (2000) found that the abnormal recovery of lath structure occurred at a stress less than 100 MPa. Therefore, the observation by Suzuki *et al.* (2000) seems to correspond to the case where subboundaries cannot escape from the pinning of precipitates unless the carbides grow gradually and their carbide spacing increases.

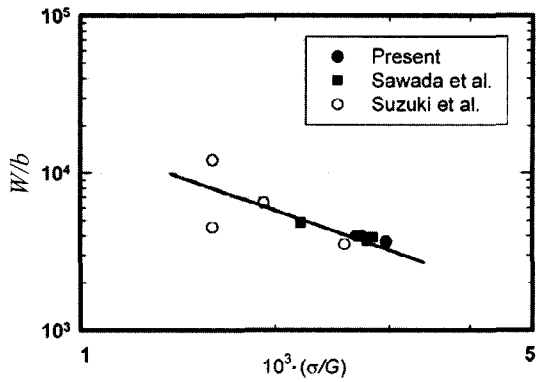

Figure 12. Relational between normalized subgrain size (W/b) at $t/t_r = 1$ and normalized stress (σ/G).

Figure 12 shows the normalized subgrain size (W/b) at $t/t_r = 1$ plotted against normalized stress (σ/G). Except for the data at the lowest stress, almost all the data points fall around a single line expressed in the form $(W/b) = m\,(G/\sigma)$, where m is 16.3. In the case of single phase materials, an analysis of many sets of data shows the similar relation with a constant of about 20. This means that the average subgrain size of a Mod.9Cr-1Mo steel is close to that of single phase materials above 137 MPa ($\sigma/G = 2.19 \times 10^{-3}$). In contrast to data points obtained above 137 MPa , the subgrain size obtained at 100 MPa is somewhat different in behavior. Actually, Suzuki *et al.* (2000) pointed out that the relation between the area fraction and subgrain size exhibited a normal distribution above 100 MPa, but it changed to the distribution with two peaks, at 7 μm^2 and 1 μm^2 at 100 MPa. This is why only some fraction of the subgrains exhibited an abnormal subgrain growth at 100 MPa. In fact, the smaller grain size at 100 MPa is much smaller than that expected from the data above 120 MPa. This fact demonstrates that most of subgrains failed to attain the final subgrain size even at $t/t_r = 1$. In other words, this fact claims that the most of

the subgrain boundaries failed to escape from the pinning of precipitates at 100 MPa. Further studies are required on the relation among *Z* phase appearing at low stresses, abnormal subgrain growth and Ostwald ripening of carbides during creep.

5. CONCLUSIONS

Aiming at the understanding of structural degradation during creep, interrupted creep tests, measurements of Vickers hardness and TEM observation have been carried out on a Mod.9Cr-1Mo steel at 873 to 923 K and 71 to 167 MPa. Results obtained in the present study are as follows;

(1) The structure of the Mod.9Cr-1Mo steel was thermally stable in static aging. But the structural degradation was accelerated by creep strain.
(2) The change in Vickers hardness was expressed as a function of creep life consumption ratio in the form of Equation (1) in the text.
(3) The change of tempered lath width was expressed as a function of creep strain in the form of Equation (3).
(4) The increase of lath width with creep strain was explained in analogy with the theory of grain growth driven by the change of interfacial energy.
(5) A model describing the relation between hardness and creep life consumption ratio was proposed. The model suggests that about 65% of hardness loss is due to the decrease of dislocation density accompanied by the movement of lath boundaries.
(6) The role of carbides along lath boundaries was discussed in connection with normal and abnormal subgrain growth during creep.

REFERENCES

ASME Boiler and Pressure Vessel Code, Case 1934. Seamless Modified 9Cr-1Mo Section I.

ASTM A213-83.

Bursik, O., J., Kucharova, K and Sklenicka, V. (1998). Microstructural development during high temperature creep of 9%Cr steel. *Mater. Sci. Eng.*, **A245,** 39.

Cerri, E., Evangelista, E., Spigarelli, S. and Bianchi, P. (1998). Evolution of microstructure in a modified 9Cr-1Mo steel during short term creep. *Mater. Sci. Eng.*, **A245,** 285.

Endo, T. and Shi, J. (1994). Strength of materials. Ed. by H. Oikawa, K. Maruyama, S. Takeuchi and M. Yamaguchi, *JIM*, 665.

Excell, S. F. and Warrington, D. H. (1972). Sub-grain boundary migration in aluminium. *Phil. Mag.* **26,** 1121.

Fukutomi, H. and Horiuchi, R. (1979). Stress induced migration of <112> symmetric tilt boundaries. *J. Japan Inst. Metals*, **43,** 1025.

Fukutomi, H. and Horiuchi, R. (1981). Stress induced migration of <112> and <100> symmetric tilt boundaries. *J. Japan Inst. Metals*, **45,** 574.

Hillert, M. (1965). On the theory of normal and abnormal grain growth. *Acta Met.*, **13,** 227.

Kouon Henkei Tokusei Deta Shyu. (1992). ISIJ, Tokyo, 117.

Kushima, H., Kimura, K. and Abe, F. (1999). Degradation of Mod.9Cr-1Mo Steel during long-term creep deformation. *Tetsu-to Hagane*, **85,** 841.

Masuyama, F. and Nishimura, N. (1994). Srength of Materials. Ed. by H. Oikawa, K. Maruyama, S. Takeuchi and M. Yamaguchi. *JIM*, 657.

Nishizawa, T., Ohmura, I. and Ishida, K. (1977). Examination of the Zener relationship between grain size and particle dispersion. *Mater. Trans. JIM*, **38,** 950.

Park, K. S., Masuyama, F. amd Endo, T. (2001). Creep modeling for life evaluation of heat-resistant steel with a martensitic structure. *ISIJ International*, **41,** S 86–90.

Park, K. S., Masuyama, F. and Endo, T. (1998). Short-term creep behavior analysis of a Mod.9Cr-1Mo steel. *Tetsu-to Hagane*, **84,** 526–533.

Park, K. S., Masuyama, F. and Endo, T. (1999). Constitutive equation describing creep curve of a statically aged Mod.9Cr-1Mo steel. *J. Japan Inst. Metals*, **63,** 597.

Park, K. S., Masuyama, F. and Endo, T. (1999). Improvement of Ω method to estimate creep behavior of a Mod.9Cr-1Mo steel. *Tetsu-to Hagane*, **85,** 492.

Prager, M. (1994). Strength of materials. Ed. by H. Oikawa, K. Maruyama, S. Takeuchi and M. Yamaguchi, *JIM*, 571.

Read, W. T., Jr. (1953). *Dislocations in Crystls.* McGraw-Hill. New York. 155.

Sandstrom, R. and Konyr, A. (1972). *Model for Tertiary-creep in Mo-and CrMo-Steels.* ICM3. Cambridge. UK. **2.** 275.

Sawada, K., Maruyama, K., Hasegawa, Y. and Muraki, T. (1999). *Creep and Fracture of Engineering Materials and Structures.* Ed. by T. Sakuma, K. Yagi, Trans Tech Publications. Swiss. 109–114.

Sawada, K., Maruyama, K., Komine, R. and Nagae, Y. (1997). Microstructural changes during creep and life assessment of Mod.9Cr-1Mo steel. *Tetsu-to-Hagane*, **83,** 466–471.

Sawada, K., Takeda, M., Maruyama, K., Komine, R. and Nagae, Y. (1998). Residual creep life assessment by change of martensitic lath structure in modified 9Cr-1Mo steels. *Tetsu-to-Hagane*, **84,** 580.

Suzuki, K., Kumai, S., Kushima, H., Kimura, K. and Abe, F. (2000). Heterogeneous recovery and precipitation of Z phase during long term creep deformation of modified 9Cr-1Mo steel. *Tetsu-to Hagane*, **86,** 550.